Astronomical Techniques and Instruments, Vol. 3, January 2026, 82–91

Article Open Access

Progress in VLBI observations with the Haoping 40 m radio telescope

De Wu[1], Jintao Luo[2*], Yue Hu[1,3], Wu Jiang[4], Zhen Yan[4], Jia Liu[1], Rurong Chen[5], Lang Cui[6], Yuping Gao[1,3], Wen Chen[7], Pingli Wang[1], Yifeng Li[1,3], Zurong Zhou[1]

[1]*National Time Service Center*, *Chinese Academy of Sciences*, *Xi'an* 710600, *China*

[2]*Qianyuan Laboratories*, *Hangzhou* 310000, *China*

[3]*University of Chinese Academy of Sciences*, *Beijing* 100049, *China*

[4]*Shanghai Astronomical Observatory*, *Chinese Academy of Sciences*, *Shanghai* 200030, *China*

[5]*National Astronomical Observatories*, *Chinese Academy of Sciences*, *Beijing* 100101, *China*

[6]*Xinjiang Astronomical Observatory*, *Chinese Academy of Sciences*, *Urumqi* 830011, *China*

[7]*Yunnan Observatories*, *Chinese Academy of Sciences*, *Kunming* 650216, *China*

*Correspondence: jluo@ntsc.ac.cn

Received: March 18, 2025; Accepted: July 8, 2025; Published Online: July 9, 2025; https://doi.org/10.61977/ati2025035; https://cstr.cn/32083.14.ati2025035

Citation: Wu, D., Luo, J. T., Hu, Y., et al. 2026. Progress in VLBI observations with the Haoping 40 m radio telescope. *Astronomical Techniques and Instruments*, **3**(1): 82−91. https://doi.org/10.61977/ati2025035.

Abstract: The Haoping 40 m radio telescope at the National Time Service Center, Chinese Academy of Sciences was built in 2014 and is primarily used to observe navigation satellites and pulsars. Since the first successful very long baseline interferometry (VLBI) observation of L-band radio source fringes in 2022, ten observations have been made so far. The stations involved in the observations include the Haoping 40 m radio telescope (Haoping), the Tianma 65 m radio telescope (Tianma), the Nanshan 26 m radio telescope (Urumqi), the Guizhou 500 m radio telescope (FAST), the Jilin 13 m radio telescope (Jilin), the Effelsberg 100 m radio telescope (Effelsberg), the Onsala 25 m radio telescope (Onsala), and the Chiang Mai 40 m radio telescope (Chiang Mai). This paper presents details on the specifications of the Haoping 40 m radio telescope, as well as the design of the VLBI experiment, the observation process, and the data processing. We also discuss the analysis of the fringe results involving the Haoping 40 m radio telescope, using Distributed FX Correlator to obtain excellent results. We confirm that the telescope is capable of participating in VLBI observations and performing specific data processing tasks. It can therefore play a greater role in future VLBI observations.

Keywords: VLBI; Radio Telescope; Distributed FX Correlator; Fringe fitting; Pulsar

1. INTRODUCTION

The Haoping 40 m radio telescope (HPRT) was constructed in 2014 at Haoping station in Luonan County, China, approximately 100 km east of Xi'an. Although surrounded by mountains, its view is largely unobstructed, and the superior local electromagnetic environment is highly conducive to radio astronomical observations. It currently plays an important role in satellite observations, pulsar observations, and VLBI observations at the National Time Service Center, Chinese Academy of Sciences (NTSC)[1–3].

VLBI yields exceptionally high-precision angular measurements and is among the observational techniques with the highest angular resolution in astronomy. It has a wide range of applications in astrometry, geodesy, and deep space navigation[4–6], as well as in the study of time comparison methods[7]. Currently, the Chinese VLBI Network (CVN) includes the Beijing 50 m radio telescope (Beijing), Sheshan 25 m radio telescope (Sheshan), Tianma 65 m radio telescope (Tianma), Nanshan 26 m radio telescope (Urumqi), and Kunming 40 m radio telescope (Kunming). These telescopes play an important role in international geodesy, astrometry, astrophysics, and Chinese deep space exploration projects. Telescopes usable as VLBI stations are widely distributed internationally, with VLBI networks including the European VLBI Network (EVN), the Very Long Baseline Array (VLBA) in the USA, the East Asian VLBI Network (EAVN), and the Long Baseline Array (LBA) in Southern Australia[8–10], as well as the International VLBI Service for Geodesy and Astrometry (IVS). IVS is mainly responsible for coordinat-

ing and organizing geodetic VLBI stations around the world to participate in observations, data transmission, correlation and post-processing, and data analysis. The results of these observations are mainly utilized for calculating Universal Time (UT1), Earth Orientation Parameters (EOP), and the measurement of the celestial reference frame. Several other stations based in China also participate in the VLBI observations organized by IVS[11,12].

The antenna of the HPRT (shown in Fig. 1) uses a Cassegrain configuration. Its main reflector is constructed from multiple solid panels spliced together, with an azimuth-elevation rotation type. The panel accuracies of the main reflector and sub-reflector are better than 0.6 mm and 0.15 mm, respectively.

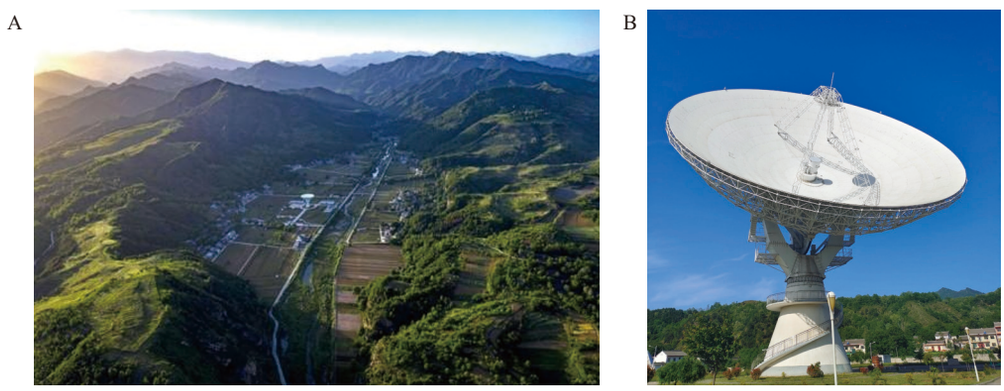

Fig. 1. The HPRT at Haoping station. (A) Overhead view of the park. (B) Side view of the telescope.

2. EXPERIMENT

2.1. Observation Equipment

The observation equipment at the Haoping station includes an antenna, pulsar signal processing equipment, and VLBI signal processing equipment. Detailed parameters of the HPRT are presented in Table 1, which has four receivers operating in the L-, S-, C-, and X-bands[13]. The L-band receiver is mainly used for VLBI and pulsar observations; it is the most frequently used receiver on the HPRT, with an observational frequency range of 1.10–1.75 GHz. The C-band receiver is a broadband cryogenic receiver with an observational frequency range of 3.6–7.2 GHz. It was installed in August 2024.

Table 1. Key parameters of the HPRT

Parameters	Value
Antenna diameter/m	40
Antenna types	Cassegrain parabolic antenna
Antenna rotation range	Azimuth: −320° to 320° (relative to south); Elevation: 5°–90°
Maximum slew rates/(°/s)	Azimuth: 1.5; Elevation: 1
Minimum speed/(°/s)	0.0005
Pointing accuracy	⩽ 1/10 beam width
Main reflector panel accuracy/mm	⩽ 0.6
Sub-reflector panel accuracy/mm	⩽ 0.15
Frequency bands	L, S, C, X

Fig. 2 shows the VLBI equipment at Haoping station. Fig. 2A is the data acquisition system, Digital Base-Band Converter 3 (DBBC3), which can provide 1–8 intermediate frequencies (IFs). The maximum bandwidth of each IF is 4 GHz, and it can generate a maximum data rate of 16 to 128 Gbps when using 2-bit sampling[14]. The DBBC3 has been installed at Haoping station, but has not yet officially started operation. Fig. 2B is the data storage server, where all the data collected by VLBI observations at Haoping station are recorded. Fig. 2C is the time and frequency system, including a multi-channel high-precision time interval measuring instrument, a pulse distributor, and a high-performance rubidium clock[15]. Fig. 2D is the Mark6 system, which has a maximum recording rate of 16 Gbps and supports the Mark5B and VLBI Data Interchange Format (VDIF) data formats commonly used in astronomy[16]. Fig. 2E shows the VLBI backend system currently in use at Haoping station, including the Chinese VLBI Data Acquisition System 2 (CDAS2) and an industrial computer used to control it. CDAS2 supports a maximum of 512 MHz IF inputs with 16 baseband channel outputs, and also supports the output of data in Mark5B format[17–19]. Fig. 2F shows the downconverter, including the L-band downconverter, X-band downconverter, and C-band downconverter. Currently, the L-band downconverter is used for VLBI observations, and the X-band down-

converter is still being tested. In addition, the device used to measure the clock offset at Haoping station is a multi-channel 53220A-350M universal frequency counter, which measures the clock difference offset between the Global Positioning System (GPS) receiver time and local cesium clock time.

Fig. 2. Photographs of the VLBI observation equipment at Haoping station. (A) VLBI digital backend. (B) Data storage servers. (C) Time and frequency system. (D) Mark6 VLBI data recording system. (E) VLBI backend system. (F) Downconverter.

2.2. VLBI Network

After starting operation in 2023, the HPRT has officially participated in a series of VLBI observations, with observation targets including radio sources and satellites. The VLBI stations participating in these observations are all located across Asia and Europe, with the geographical distribution shown in Fig. 3, including five Chinese stations, one German station, one Swedish station, and one Thai station. Detailed information about the stations is presented in Table 2.

2.3. Overview of Observations

In 2022, the HPRT participated, for the first time, in a VLBI test observation organized by the Shanghai Astronomical Observatory, Chinese Academy of Sciences (SHAO), together with the Tianma telescope at the SHAO and the Urumqi telescope at the Xinjiang Astronomical Observatory, Chinese Academy of Sciences. On June 22, long baseline fringes were successfully obtained on the Tianma-Haoping and Urumqi-Haoping baselines, confirming the ability of the HPRT to carry out VLBI observations.

From April 2023 to August 2024, the HPRT officially participated in a series of fringe tests and astrometric observations, with observation durations ranging from 0.6 h to 6.7 h, organized by the SHAO, the Guizhou Radio Astronomical Observatory, and the NTSC[20], and a summary of the VLBI observations in which the HPRT participated is given in Table 3. From 2023 to 2024, the HPRT participated in a total of ten VLBI observations, including eight radio source observations and two satellite observations, all conducted in the L-band.

A total of 28 target sources and 6 satellites were

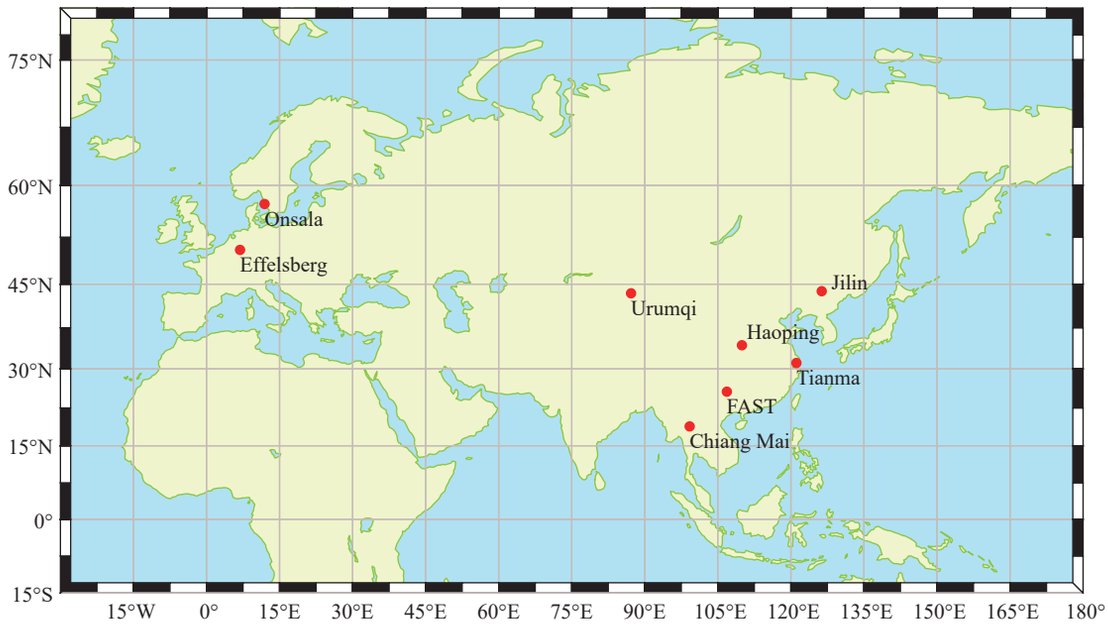

Fig. 3. Distribution of radio observatories participating in VLBI observations with the HPRT.

Table 2. Technical details about VLBI stations

Station name	Antenna diameter/m	Country	Number of observations
Haoping	40	China	10
Tianma	65	China	4
Urumqi	26	China	5
FAST	500	China	5
Jilin	13	China	3
Effelsberg	100	Germany	1
Onsala	25	Sweden	1
Chiang Mai	40	Thailand	1

Table 3. Statistics of experimental VLBI observations involving HPRT

Date (yyyy−mm−dd)	Duration/h	Type	Stations
2023−04−11	6.0	Radio source observation	Haoping, Tianma, Urumqi, FAST
2023−11−13	5.7	Radio source observation	Haoping, Tianma, Urumqi
2023−11−29	6.7	Radio source observation	Haoping, Tianma, Urumqi, FAST, Effelsberg, Onsala
2024−04−15	2.0	Radio source observation	Haoping, Urumqi, FAST
2024−04−24	0.6	Satellite ovservation	Haoping, Jilin
2024−06−10	0.8	Radio source observation	Haoping, FAST, Chiang Mai
2024−06−12	0.9	Satellite ovservation	Haoping, Jilin
2024−06−12	0.6	Radio source observation	Haoping, Jilin
2024−08−20	1.0	Radio source observation	Haoping, Tianma, Urumqi
2024−08−20	2.2	Radio source observation	Haoping, FAST

observed in the experiments, and the distribution of these target sources and satellites on the celestial sphere is shown in Fig. 4. All the target sources and satellites are located in the northern celestial sphere or near the celestial equator, making them more favorable for an array of stations located in the northern hemisphere.

2.4. Observation Design

Before each observation, the required target sources and observation time periods are selected according to the task requirements, and the observation frequency, bandwidth, upper and lower sidebands, and bit sampling parameters are configured according to the parameters of the participating stations. The Sked software is used to compile the observation outline file based on these parameters, i.e. a VLBI experiment format (VEX) file[21]. This file is the overall input file for the VLBI system, and it must ensure that the radio telescopes forming one or more baselines

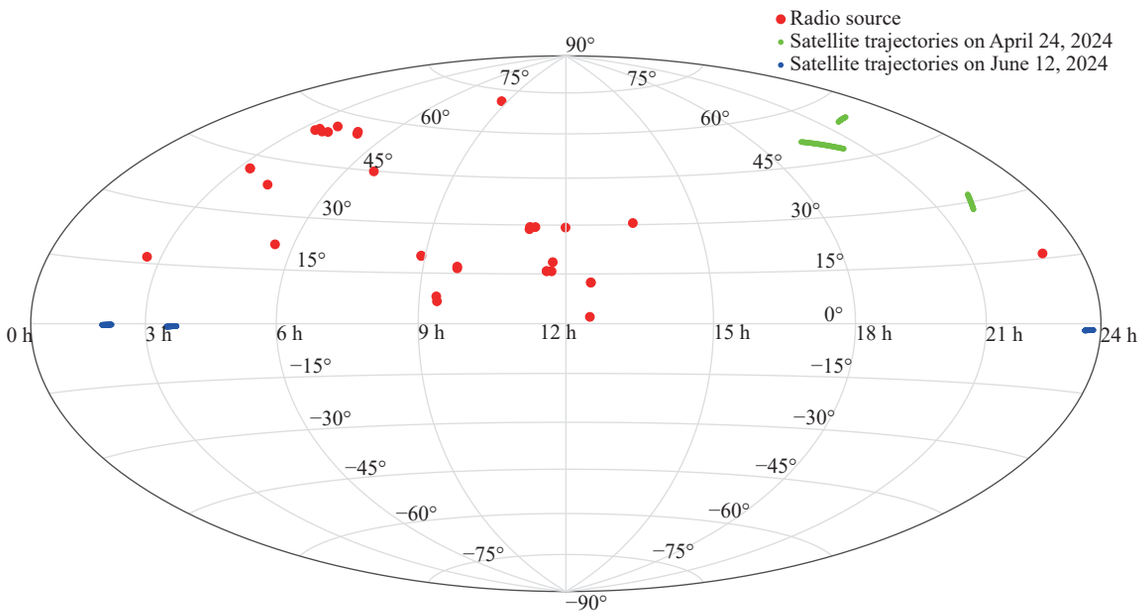

Fig. 4. Map of the celestial sphere, showing observed radio sources and satellites. The numbers on the horizontal line show declination, and the numbers on the vertical line show right ascension.

are pointed at the same source in the same time period. Furthermore, the data recording must be synchronized. The observation outline typically needs to be prepared a few weeks prior to the actual observation, and usually contains several configuration parameters related to the observation, and includes antenna parameters, IF parameters, frequency parameters, data format parameters, source parameters, and scan parameters.

Taking the clp23a observation as an example (i.e. the first CVN observation of 3 pulsars in the L-band during 2023), which was a phase-referenced pulsar VLBI observation, with two calibrators as well as three target sources and three phase-referenced sources. The observation was set up with 4 Baseband converter (BBC) channels with central frequencies of 358.00 MHz, 400.00 MHz, 432.00 MHz, and 464.00 MHz, with a bandwidth of 32 MHz and 2-bit sampling.

2.5. VLBI Observation and Signal Processing

The VLBI observation process at the HPRT is shown in Fig. 5. The first step is to formulate the observation task according to the observation outline, including the task name, start and end times, and the frequency band of the observation. Subsequently, based on the intended target sources and time period, the azimuth and elevation of the antenna are calculated every second. The clock offset at Haoping station is determined by the difference between the GPS signal and the local cesium clock, which must be calibrated before the observation; the clock offset value can be displayed on the frequency counter. It is also necessary to open the current signal channel and adjust the attenuation value. The next step is to check the configuration parameters of the CDAS2 and import the VEX file into the CDAS2, to automatically identify the relevant parameters or manually set the parameters of the CDAS2, including the IF frequency of each frequency channel, the upper or lower sidebands, the polarization, and the bandwidth. Bit sampling information must be synchronized with the local time server (Network Time Protocol, NTP). Finally, a strong radio source must be used to test the signal.

The VLBI signal flowchart for Haoping station is shown in Fig. 6. After the observation begins, the radio signal received by the radio telescope (a pulsar in this example) converges to the feeder through the antenna reflecting surface, and the signal output from the feeder is sent to the Low Noise Amplifier (LNA), which is converted into optical signal and transmitted to the machine room by optical fiber. It is then converted back to electrical signal through an optical transceiver, to yield the radio frequency (RF) signal. The downconverter amplifies this RF signal, then mixes it with a Local Oscillation (LO) signal to get the IF signal, and which is then sent to the CDAS2 data acquisition backend for data acquisition. The time and frequency system provides the pulse per second (PPS) signal and the 10 MHz signal for the CDAS2.

The data acquisition backend is a device that digitally samples and encodes the IF signals output by the downconverter and records them to a local disk, or transmits them directly from the network to the analysis center. In the acquisition backend, the IF signal is divided into multiple channels and converted to a base frequency signal in the range of zero to several megahertz. This is converted from bit sampling to a digital signal by an analog-to-digital (A/D) converter. The digitized signal is bound to a time scale and fed into the encoder as a digital time series, which is then recorded in the data recording server in Mark5B and VDIF format. In addition, the

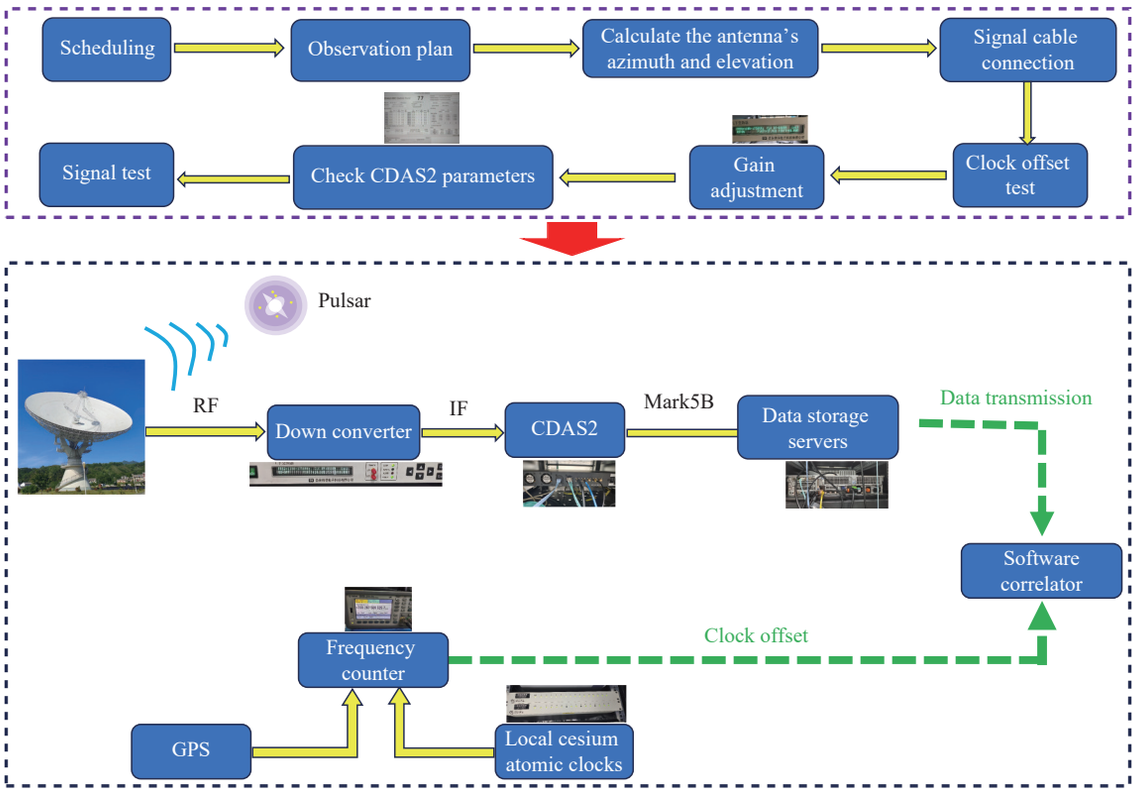

Fig. 5. Observation flowchart of VLBI at Haoping station.

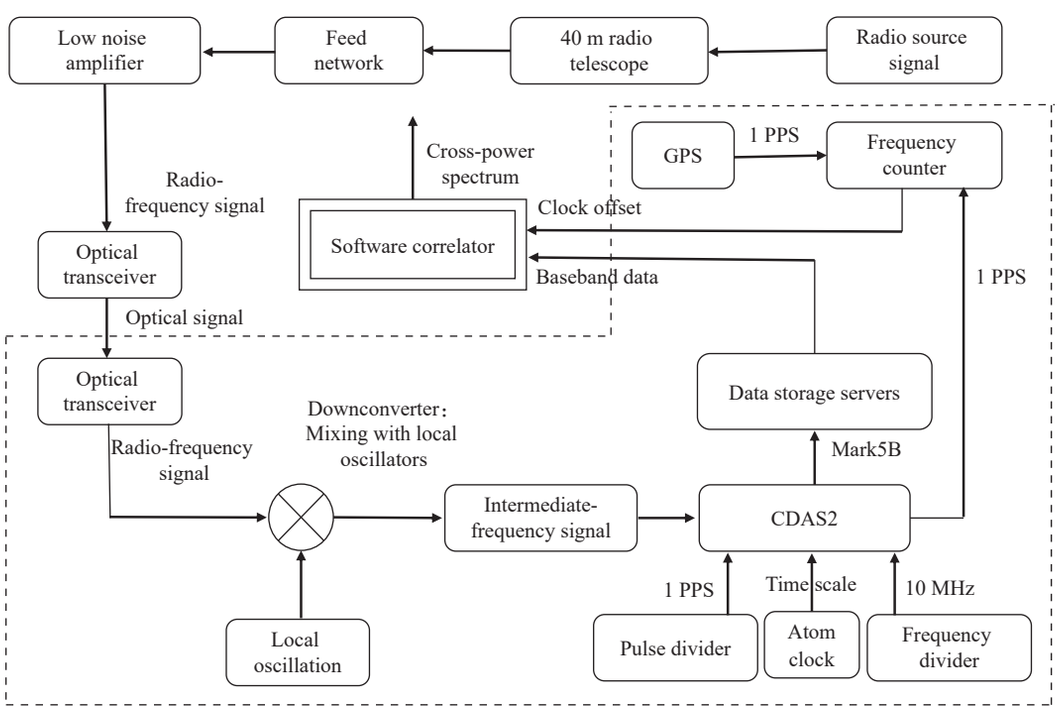

Fig. 6. Signal flowchart for VLBI at Haoping station.

1 PPS signal from the GPS and the 1 PPS signal output from the CDAS2 are fed into a frequency counter to calculate the clock offset. At the end of the observation, the data and clock offset information are correlated.

3. CORRELATION

At the end of the VLBI experiments, the data were correlated using the Distributed FX Correlator (DiFX) soft-

ware version 2.6.2[22,23], and fringe fitting was performed using the HOPS (Haystack Observatory Postprocessing System) software version 3.23[24]. When performing satellite VLBI data correlation, the delay model needs to be recalculated and replaced according to the satellite orbit. First, the job delay file is generated based on the coordinate sequence of the satellite in the geocentric inertial coordinate system. The calcif2 program is then used to generate the input model (IM) file with delay and delay rate data points at 5-second intervals, The corresponding time values in the IM-file are replaced with the delays from the job file, and then data correlation and fringe fitting are performed.

4. RESULTS AND DISCUSSION

The correlation, as well as the fringe fitting procedure, yields a map of the fringe results for each baseline. Fig. 7A shows the results of the Haoping-Urumqi baseline correlation output, which calibrates the residual delays and phases from a VLBI observation of a radio source, conducted in April 2023, in the L-band. Four upper sideband channels were configured, each with a 32 MHz bandwidth, 2-bit quantization, and a data logging rate of 128 Mbps. Fig. 7B shows the fringe results for the Haoping-Jilin baseline in a satellite VLBI observation, in June 2024, which was a satellite VLBI test observation using only one 32 MHz bandwidth channel and 2-bit quantization.

From the processing results in Fig. 7A, it can be seen that the fringe Signal-to-Noise Ratio (SNR) of the radio source at Haoping and Urumqi stations reaches 41, and the phase of the fringe of each channel is distributed on the two sides of the 0 phase. In Fig. 7B, the fringe SNR of the satellite reaches 1048. Due to the difference in the nature of the satellite signal and the radio source signal, the radio source is a white noise signal, while the satellite signal is concentrated in a certain frequency interval, with a central frequency point[25], therefore, it can be seen that there exists a peak in the fringe amplitude from the figure, and the phase is also a relatively flat near this peak.

5. SUMMARY and OUTLOOK

This paper introduces the progress in VLBI observations at the HPRT in the L-band, over the past 2 years. We have included the status of other stations participating in these VLBI observations, the statistics of the observation information, the observation setups, and detailed descriptions of the general observation process of the HPRT participating in VLBI observations. We have also discussed the process and results of data correlation and fringe fitting. Currently, a complete VLBI observation process has been devised for the HPRT, allowing its successful participation in ten VLBI observations. It has also demonstrated the capability to conduct correlation and data analysis. If the HPRT is incorporated into the CVN, it can help to mitigate the uneven distribution of CVN stations and optimize the baseline configuration, while enriching and improving the UV coverage of the CVN. In aperture synthesis observations, the projection of the baseline in the plane perpendicular to the direction of the observed source is referred to as UV coverage, and the projection plane is called the UV plane. Because of the continuous motion of the target source in space, the baseline vector changes continually, resulting in UV coverage formed by projections onto the UV plane. Performing a Fourier transform on the UV coverage yields the aperture synthesis

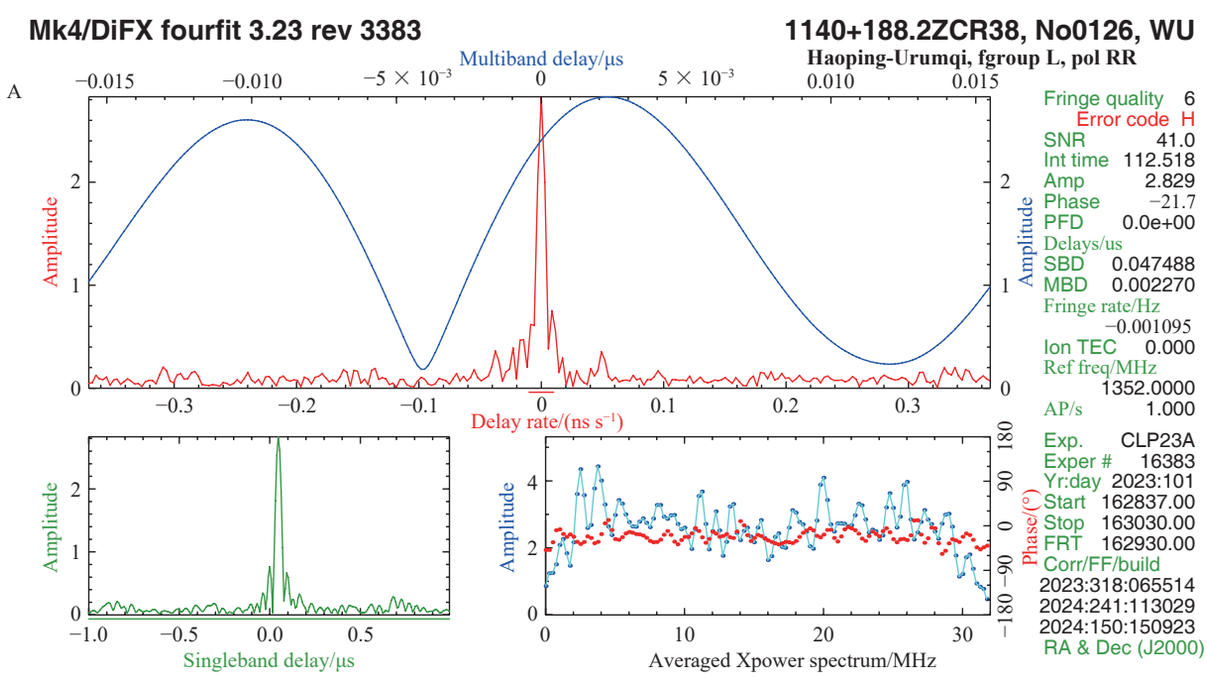

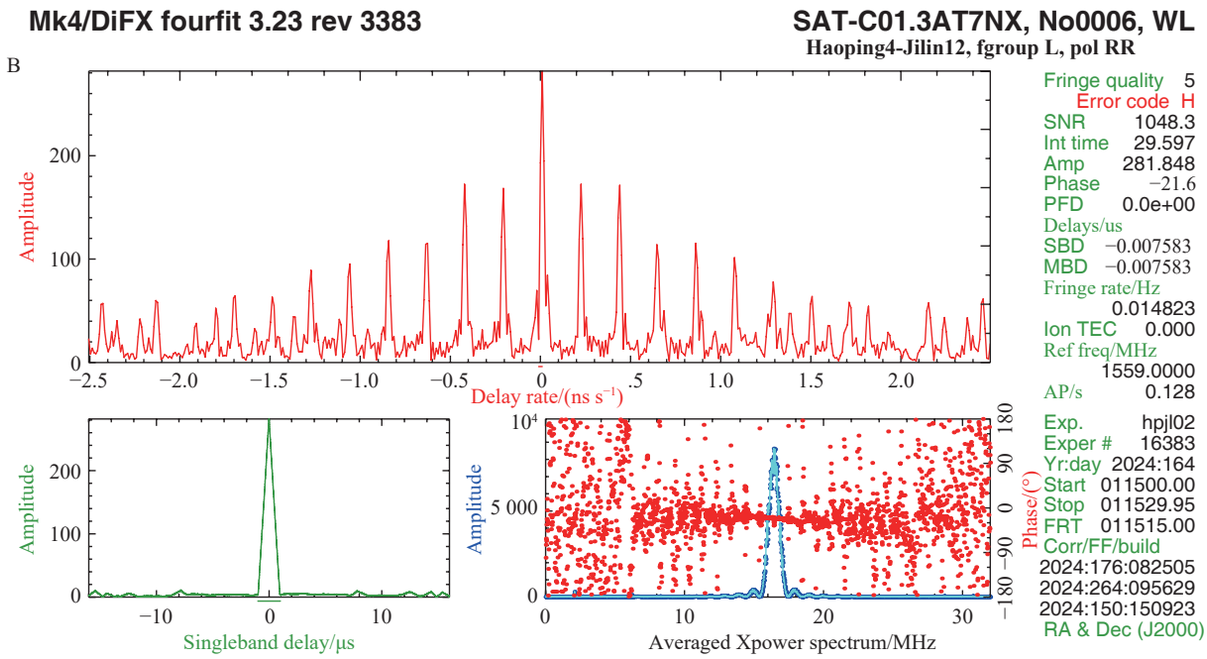

Fig. 7. Fringe fitting results at Haoping station for (A) Haoping-Urumqi, and (B) Haoping-Jilin. For each, the top panel shows delay rate (red) for the fringe search. The lower left panel shows single band delay, and the lower right panel shows fringe amplitude (blue) and fringe phase (red) for the cumulative upper and lower sideband channels.

beam. Good UV coverage is essential for obtaining an ideal antenna beam and finally determines the quality of the image. Fig. 8A shows a simulation result of the UV coverage that can currently be obtained by the CVN network, and Fig. 8B shows the UV coverage simulation results obtained after the addition of the Haoping station to the CVN. Adding the Haoping station to the CVN yielded a greater number of high-sensitivity baselines, improving the uniformity and range of UV coverage, significantly helping to improve the imaging quality.

In our future work, we will consider officially commissioning the DBBC3 digital acquisition backend on the HPRT, which can offer higher performance, together with the two Mark6 data logging systems. Compared with the CDAS2, which has a maximum recording bandwidth of only 512 MHz, the DBBC3 supports a maximum data recording bandwidth of 4096 MHz and can provide outputs ranging from 16 Gbps to 128 Gbps. The Mark6 system also maintains a sustained data recording rate of 16 Gbps, which is essential to improve the sensitivity, resolution, and frequency coverage of VLBI observations, while helping the HPRT to participate in other international joint VLBI observations, including EVN broadband recording observations.

A C-band cryogenic receiver was installed at the HPRT in August 2024, and the signal link has been tested. Fig. 9A shows the OH spectral lines of the star-forming region W3 (OH) observed by the Haoping station at 6.67 GHz in the C-band. A corresponding time and frequency system, downconverter, and data storage system have also been installed to operate in the X-band, and can be used for VLBI observations after a link test is

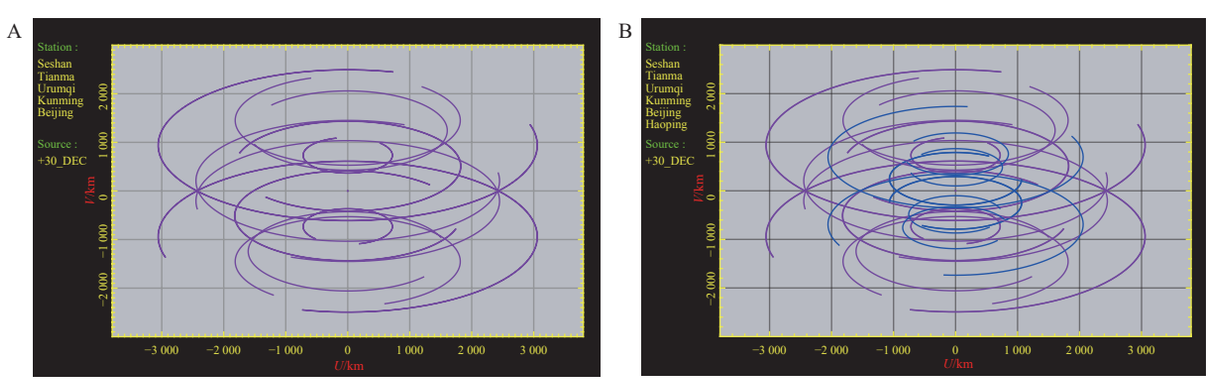

Fig. 8. UV coverage of the CVN for a source at 30° declination. The purple curve shows the UV trajectory formed by the CVN baselines, while the blue curve shows the UV trajectory formed by Haoping station and the CVN stations. (A) UV coverage obtained by the current CVN station. (B) UV coverage after Haoping station joins the CVN.

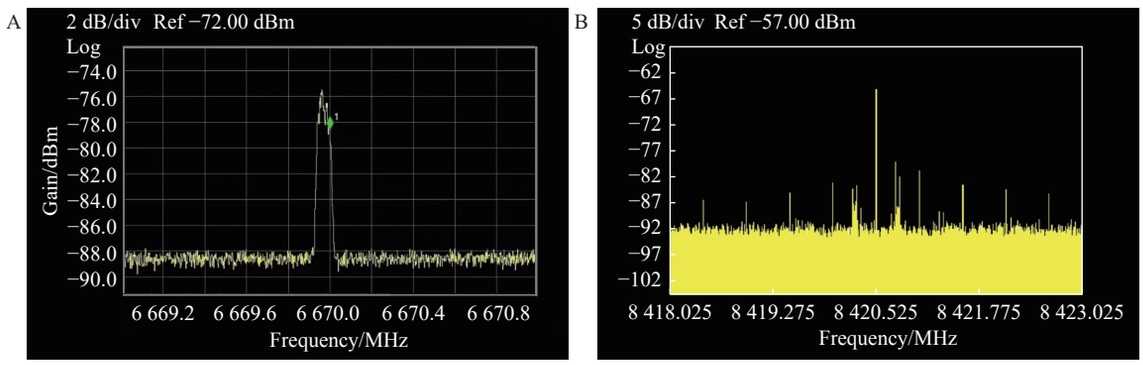

Fig. 9. C-band and X-band results observed by the HPRT. (A) W3(OH) spectral lines observed in the C-band. (B) Mars probe signals observed in the X-band.

carried out. Fig. 9B shows the signal from the European Mars Express mission, observed by the HPRT in the X-band, showing clear detections of the main carrier and sidetone signals. Downconverters have not yet been installed for the S-band, but S-band capabilities will be installed and tested in the future. The HPRT will ultimately be able to carry out VLBI observations in the L-, C-, S-, and X-bands, allowing high-precision positional measurements of pulsars and other celestial objects, station coordinate measurements, UT1 measurements, reference frame connections, studies of the interstellar medium, and other astrometric and geodetic measurements.

ACKNOWLEDGEMENTS

We thank other members of the project team for their hard work, dedication, support, and assistance. This work was supported by the National Science and Technology Major Project (E152KJ1201), the Natural Science Basic Research Program of Shaanxi (2024JC-YBQN-0036), the National Natural Science Foundation of China (42030105 and 11973046), and the National SKA Program of China (2020SKA0120200).

AI DISCLOSURE STATEMENT

ChatGPT-4.1 was employed for language and grammar checks within the article. The authors carefully reviewed, edited, and revised the Deepseek-generated texts to their own preferences, assuming ultimate responsibility for the content of the publication.

AUTHOR CONTRIBUTIONS

Jintao Luo conceived the ideas. De Wu designed and implemented the study and wrote the paper. Yue Hu collaborated with De Wu to conduct the VLBI observations at Haoping station, and Yifeng Li provided technical support. Zhen Yan organized and coordinated the VLBI observation in April 2023. Rurong Chen, Lang Cui, Jia Liu, and Wu Jiang planned and implemented these VLBI observations. Jia Liu, Yuping Gao, Wen Chen, Pingli Wang, and Zurong Zhou reviewed and edited the paper. All authors read and approved the final manuscript.

DECLARATION OF INTERESTS

The authors declare no competing interests.

REFERENCES

[1] Schuh, H., Behrend, D. 2012. VLBI: a fascinating technique for geodesy and astrometry. *Journal of Geodynamics*, **61**: 68−80.

[2] Thompson, A. R., Moran, J. M., Swenson, G. W. 2017. Interferometry and synthesis in radio astronomy. Switzerland: Springer.

[3] Dai, S., Sun, P. F., Liu, H. W., et al. 2022. The Crab pulsar glitch monitoring by the 40-meter radio telescope of the National Time Service Center. *Astronomical Research and Technology*, **19**(1): 16−20. (in Chinese)

[4] Cohen, M. H., Shaffer, D. B. 1971. Positions of radio sources from long-baseline interferometry. *The Astronomical Journal*, **76**: 91.

[5] Hinteregger, H. F., Shapiro, I. I., Robertson, D. S., et al. 1972. Precision geodesy via radio interferometry. *Science*, **178**(4059): 396−398.

[6] Qian, Z. H., Li, J. L. 2012. Application of very long baseline interferometry technology in deep space exploration. Beijing: China Science and Technology Press. (in Chinese)

[7] Wang, P. L. 2020. Research on time comparison method based on VLBI. Beijing: Doctor thesis, University of Chinese Academy of Sciences. (in Chinese)

[8] Booth, R. 2013. The origins of the EVN and JIVE: Early VLBI in Europe. In Proceedings of RTS2012.

[9] Akiyama, K., Algaba, J. C., An, T., et al. 2022. Overview of the observing system and initial scientific accomplishments of the East Asian VLBI Network (EAVN). *Galaxies*, **10** (6): 113.

[10] Petrov, L., Phillips, C., Bertarini, A., et al. 2011. The LBA Calibrator Survey of southern compact extragalactic radio sources–LCS1. *Monthly Notices of the Royal Astronomical Society*, **414**(3): 2528−2539.

[11] Schlüter, W., Behrend, D. 2007. The International VLBI Service for Geodesy and Astrometry (IVS): current capabilities and future prospects. *Journal of Geodesy*, **81**: 379−387.

[12] Wang, G. L., Xu, M. H. 2012. An analysis of UT1 determined by IVS intensive observations. *Chinese Astronomy and Astrophysics*, **36**(4): 408−416.
[13] Luo, J. T., Gao, Y. P., Yang, T. G., et al. 2020. Pulsar timing observations with Haoping radio telescope. *Research in Astronomy and Astrophysics*, **20**(7): 111.
[14] Tuccari, G., Buttaccio, S., Alef, W., et al. 2016. DBBC3: VLBI at 32 Gbits per second. In Proceedings of 11th European VLBI Network Symposium & Users Meeting, SISSA Medialab.
[15] Wang, L. L., Liu, Q. H., Cai, Y. 2024. The time and frequency system of the Tianma 65 m radio telescope. *Astronomical Techniques and Instruments*, **1**(5): 260−266.
[16] Whitney, A. R., Lapsley, D., Taveniku, M. 2011. Mark 6: a next-generation VLBI data system. In Proceedings of 20th Meeting of the European VLBI Group for Geodesy and Astronomy.
[17] Zhu, R. J., Wu, Y. J., Li, J. Y., et al. 2018. The Development of VLBI digital backend in SHAO. In Proceedings of 2018 Progress in Electromagnetics Research Symposium (PIERS-Toyama).
[18] Zhu, R. J., Wu, Y. J., Zheng, W. M., et al. 2021. Integration of very long baseline interferometry data acquisition, recording, and transmission with multichannel and multibit for CE-5 mission. *Scientia Sinica Physica Mechanica & Astronomica*, **51**(11): 119506. (in Chinese)
[19] Guo, S. G., Zhu, R. J., Zheng, W. M., et al. 2017. The progress of VLBI data acquisition system-Mark6 and related techenologies. *Astronomical Techniques and Instruments*, **14**(3): 281−287. (in Chinese)
[20] Yan, Z., Shen, Z. Q., Jiang, P., et al. 2024. Pathfinding pulsar observations with the CVN incorporating the FAST. *Chinese Physics Letters*, **41**(11): 117501.
[21] Gipson, J. 2010. An introduction to Sked. In Proceedings of the Sixth General Meeting of the International VLBI Service for Geodesy and Astrometry.
[22] Deller, A. T., Tingay, S. J., Bailes, M., et al. 2007. DiFX: a software correlator for very long baseline interferometry using multiprocessor computing environments. *Publications of the Astronomical Society of the Pacific*, **119**(853): 318.
[23] Deller, A. T., Brisken, W. F., Phillips, C. J., et al. 2011. DiFX-2: a more flexible, efficient, robust, and powerful software correlator. *Publications of the Astronomical Society of the Pacific*, **123**(901): 275.
[24] Lonsdale, C., Cappallo, R. 1996. Haystack Observatory Postprocessing System (HOPS). MIT Haystack Observatory website. Available from: https://www.haystack.mit.edu/haystack-observatory-postprocessing-system-hops/.
[25] Plank, L., Hellerschmied, A., McCallum, J., et al. 2017. VLBI observations of GNSS-satellites: from scheduling to analysis. *Journal of Geodesy*, **91**: 867−880.